doi:10.1038/nature07526

LETTERS

The insect nephrocyte is a podocyte-like cell with a filtration slit diaphragm

Helen Weavers[1]*, Silvia Prieto-Sánchez[2]*, Ferdinand Grawe[3], Amparo Garcia-López[4], Ruben Artero[4], Michaela Wilsch-Bräuninger[5], Mar Ruiz-Gómez[2], Helen Skaer[1] & Barry Denholm[1]

The nephron is the basic structural and functional unit of the vertebrate kidney. It is composed of a glomerulus, the site of ultrafiltration, and a renal tubule, along which the filtrate is modified. Although widely regarded as a vertebrate adaptation[1], 'nephron-like' features can be found in the excretory systems of many invertebrates, raising the possibility that components of the vertebrate excretory system were inherited from their invertebrate ancestors[2]. Here we show that the insect nephrocyte has remarkable anatomical, molecular and functional similarity to the glomerular podocyte, a cell in the vertebrate kidney that forms the main size-selective barrier as blood is ultrafiltered to make urine. In particular, both cell types possess a specialized filtration diaphragm, known as the slit diaphragm in podocytes or the nephrocyte diaphragm in nephrocytes. We find that fly (*Drosophila melanogaster*) orthologues of the major constituents of the slit diaphragm, including nephrin, NEPH1 (also known as KIRREL), CD2AP, ZO-1 (TJP1) and podocin, are expressed in the nephrocyte and form a complex of interacting proteins that closely mirrors the vertebrate slit diaphragm complex. Furthermore, we find that the nephrocyte diaphragm is completely lost in flies lacking the orthologues of nephrin or NEPH1—a phenotype resembling loss of the slit diaphragm in the absence of either nephrin (as in human congenital nephrotic syndrome of the Finnish type, NPHS1) or NEPH1. These changes markedly impair filtration function in the nephrocyte. The similarities we describe between invertebrate nephrocytes and vertebrate podocytes provide evidence suggesting that the two cell types are evolutionarily related, and establish the nephrocyte as a simple model in which to study podocyte biology and podocyte-associated diseases.

Filtration of blood in the vertebrate kidney occurs within the glomerulus of the nephron (Fig. 1a, b). The filtration barrier is formed by podocytes—specialized epithelial cells—which send out interdigitating foot processes to enwrap the glomerular capillaries. These processes are separated by 30–50-nm-wide slit pores spanned by the slit diaphragm[3,4], which, together with the glomerular basement membrane, form a size- and charge-selective filtration barrier (Fig. 1b). Disruption to this barrier in disease leads to leakage of blood proteins into the urinary space and to kidney failure[5].

Although invertebrate excretory systems are considered to lack nephrons, 'nephron-like' components, such as filtration cells and ducts in which the filtrate is modified, are widespread (Fig. 1c)[6,7]. Insect nephrocytes regulate haemolymph composition by filtration, followed by endocytosis and processing to sequester and/or secondarily metabolise toxic materials[7–9]. *Drosophila* have two types of nephrocytes: garland and pericardial nephrocytes (Fig. 1e–g). They are tethered to the oesophagus (Figs 1g, 2d and 3g) or heart (Fig. 1f), and are bathed in haemolymph. Extensive infolding of the plasma membrane generates a network of labyrinthine channels or lacunae flanked by nephrocyte foot processes (Fig. 1h). The channel entrances are narrow slits 30 nm in width, spanned by a single or double filament forming a specialized filtration junction—the nephrocyte diaphragm (Figs 1h, i and 3c). Each nephrocyte is enveloped by the basement membrane (Figs 1h and 3c). The nephrocyte diaphragm and basement membrane behave as a size- and charge-selective barrier[7,9] (Fig. 1d) and filtrate is endocytosed from the sides of the lacunae. Thus, the anatomies of the nephrocyte and podocyte filtration barriers are remarkably similar[3].

In view of this similarity, we investigated whether the nephrocyte diaphragm is molecularly related to the slit diaphragm. The major slit diaphragm components, the transmembrane immunoglobulin-domain superfamily proteins nephrin and NEPH1, are co-expressed in the podocyte and interact across the slit pore by homo- and heterotypic binding to form the diaphragm[4,10–16]. Mutations in *NPHS1*, as in human congenital nephrotic syndrome of the Finnish type[10], or in *NEPH1* (ref. 17) cause slit diaphragm loss and foot process effacement, resulting in breakdown of the filtration barrier and proteinuria.

Drosophila has two *NPHS1* orthologues—*sticks and stones* (*sns*) and *hibris* (*hbs*)—and two *NEPH1* orthologues—*dumbfounded* (*duf*, also known as *kirre*) and *roughest* (*rst*; Supplementary Table 1). Because *hbs* and *rst* are expressed in only a subset of nephrocytes (data not shown), we focus on *sns* and *duf*. Sns and Duf are expressed throughout life in both nephrocyte types (Figs 2a–g, adult data not shown), from mid-embryogenesis for garland cells (Supplementary Fig. 1 and Fig. 2a, b) and from the first larval instar for pericardial cells (Fig. 2c). Interestingly, the onset of Sns and Duf expression correlates in time with the appearance of the nephrocyte diaphragm at the ultrastructural level[18,19]. Both proteins localize to the plasma membrane (Fig. 2d–g) and double-labelling reveals precise co-localization (Fig. 2h). This finding is initially surprising because in most contexts Sns and Duf are expressed in complementary patterns and mediate interactions between cells of different types. The only other situation in which the two types of immunoglobulin-domain proteins are co-expressed in the same cell is the vertebrate podocyte[14]. We find that Sns and Duf are dependent on each other for stabilization at the plasma membrane. Loss or knockdown of either protein in embryonic (Fig. 2i–l) or larval (Fig. 2m–p) nephrocytes leads to a loss, severe reduction or mislocalization of the other. These data demonstrate an essential interaction between the two proteins in the same cell, similar to that between nephrin and NEPH1 in the podocyte[13–16]. The precise subcellular location of the proteins was revealed by immuno-electron microscopy. Both Sns and Duf specifically localize to the nephrocyte diaphragm (Fig. 2q–s) and

[1]Department of Zoology, University of Cambridge, Downing Street, Cambridge CB2 3EJ, UK. [2]Centro de Biología Molecular Severo Ochoa, CSIC, UAM, Cantoblanco, 28049 Madrid, Spain. [3]Institut für Genetik, Heinrich-Heine-Universität, Düsseldorf D-40225, Germany. [4]Department of Genetics, University of Valencia, Burjasot, Valencia 46100, Spain. [5]Max Planck Institute of Molecular Cell Biology and Genetics, Dresden D-01307, Germany.
*These authors contributed equally to this work.

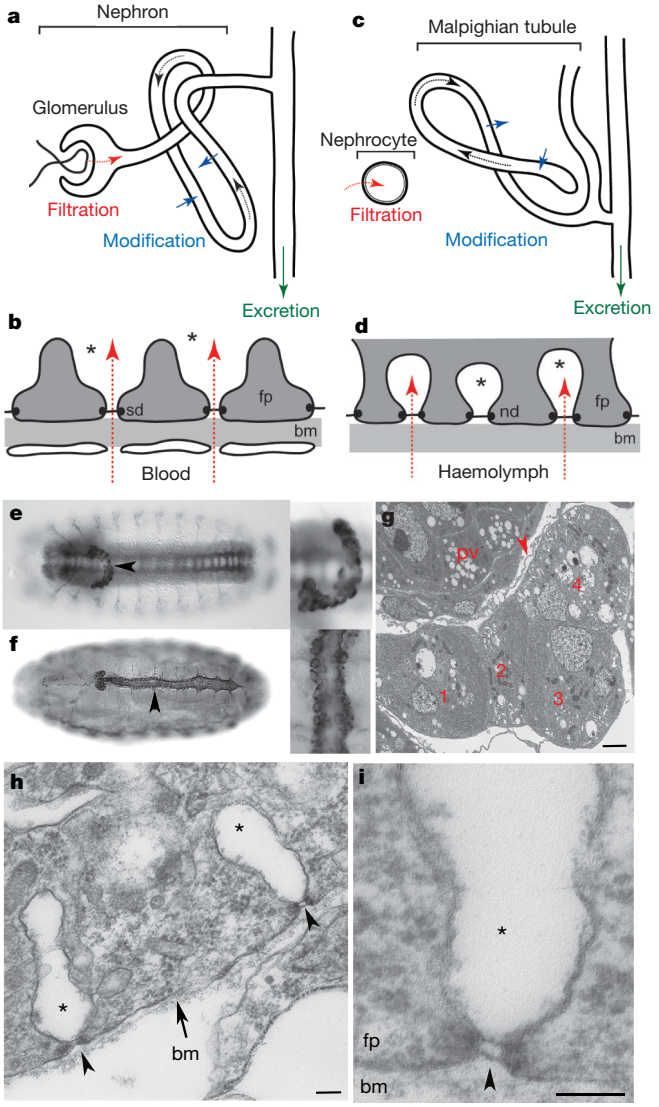

Figure 1 | The glomerular and nephrocyte filtration barriers are anatomically similar. **a**–**d**, Schematic drawings of the vertebrate nephron (**a**), glomerular filtration barrier (**b**), insect excretory system (**c**) and nephrocyte filtration barrier (**d**). Ultrafiltration (red arrow), filtrate flow (black arrow) and urinary space (**b**, asterisk) or extracellular lacunae (**d**, asterisk) are shown. bm, basement membrane; fp, foot process; nd, nephrocyte diaphragm; sd, slit diaphragm. **e**, **f**, *Drosophila* garland (anti-HRP, **e**) and pericardial (anti-pericardin, **f**) nephrocytes. Higher magnification images are shown to the right. **g**–**i**, Transmission electron micrographs of stage-16 embryonic garland nephrocytes. **g**, Four garland nephrocytes surrounding the proventiculus (pv); connective fibres (arrowhead). **h**, **i**, High magnification of the garland nephrocyte cell surface (**h**) and nephrocyte diaphragm (**i**) showing the nephrocyte diaphragm (arrowhead) and extracellular lacunae (asterisk). Scale bars: 2 μm (**g**) and 100 nm (**h**, **i**).

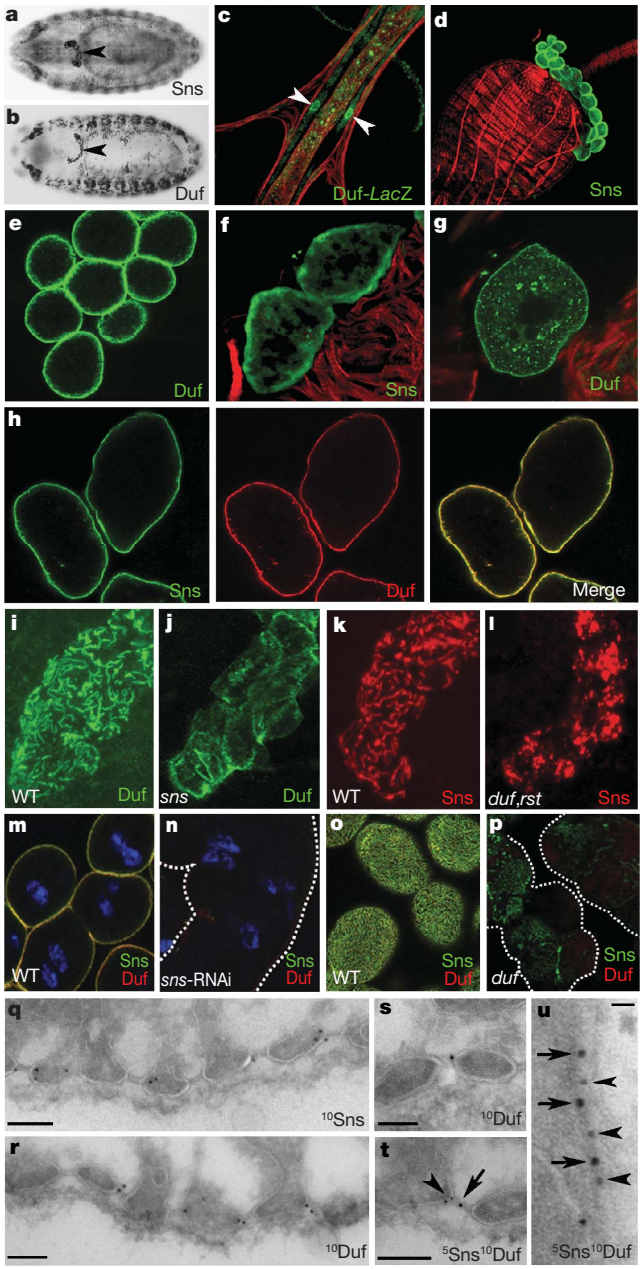

Figure 2 | Sns and Duf are expressed in *Drosophila* nephrocytes. **a**–**h**, Sns (**a**, **d**, **f**, **h**) and Duf (**b**, **c**, **e**, **g**, **h**) expression in garland (**a**, **b**, **d**, **e**) and pericardial (**c**, **f**, **g**, **h**) nephrocytes. Embryonic (**a**, **b**, arrowheads), first instar larva (**c**, green, arrowheads) and third instar larvae (**d**–**h**). The actin cytoskeleton has been counterstained in **c**, **d**, **f** and **g** (red). **h**, Sns (left, green) and Duf (centre, red) co-localize (right, yellow). **i**–**l**, Clusters of ~6–8 wild-type (WT; **i**, **k**), *sns* (**j**) or *duf,rst* (**l**) embryonic garland cells stained with anti-Duf (**i**, **j**) or anti-Sns (**k**, **l**). **m**–**p**, Wild-type (**m**, **o**), *sns*-RNAi (**n**) and *duf* (**p**) third instar garland cells stained for anti-Duf (red), anti-Sns (green; merge appears yellow) and DNA (blue). Single optical section (**m**, **n**) or *z*-projection of cell surface (**o**, **p**) are shown. **q**–**u**, Transmission electron micrographs of wild-type third instar garland cells immunogold-stained for anti-Sns (^{10}Sns, **q**) or anti-Duf (^{10}Duf, **r**, **s**), or that were double labelled (**t**, **u**). For double labelling, 5 nm (arrowhead) and 10 nm (arrow) gold particles are used for Sns and Duf, respectively. Scale bars: 100 nm (**q**–**t**) and 15 nm (**u**).

double-labelling reveals close co-localization between the two proteins (Fig. 2t, u).

Garland and pericardial nephrocytes are correctly specified in *sns* and *duf* mutants (Supplementary Fig. 2a–k). However, given the importance of the immunoglobulin-domain proteins in slit diaphragm formation, we examined the ultrastructure of the diaphragm in *sns* and *duf* mutants. In wild-type garland cells, nephrocyte diaphragms and associated lacunae appear during mid-embryogenesis (Supplementary Fig. 2l), progressively increasing in number (Fig. 1h). Diaphragms densely populate the cell periphery in third instar larvae (Fig. 3c). Notably, *sns* or *duf* mutant garland cells completely lack nephrocyte diaphragms at every stage, and lacunae are rarely detected (compare Fig. 3a, b with Fig. 1i, Fig. 3c with Fig. 3d, and Supplementary Fig. 2m, n with Supplementary Fig. 2l). Occasional infoldings do form, but are never bridged by diaphragms (Fig. 3b and Supplementary Fig. 2n). Instead, the nephrocyte surface contains frequent, small patches of electron-dense subcortical material (Fig. 3a,

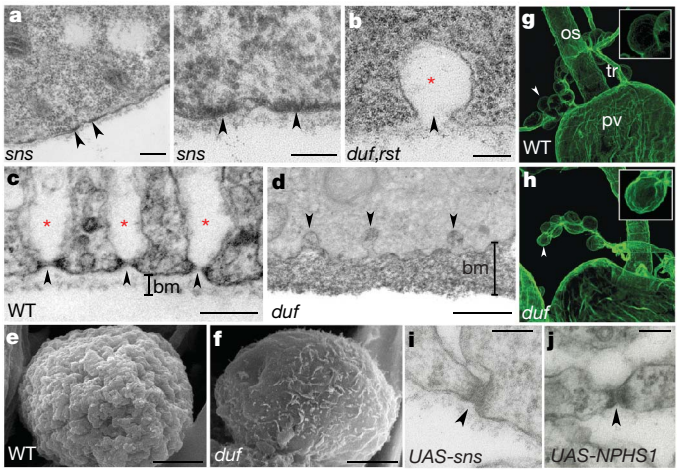

Figure 3 | Sns and Duf are required for nephrocyte diaphragm formation and normal morphology. **a**, **b**, *sns* (**a**) and *duf,rst* (**b**) embryonic garland cells lack diaphragms and lacunae. The right image of **a** is a higher magnification image of the left image, showing electron-dense subcortical material (arrowheads). Small lacunae (red asterisk) lacking diaphragms are occasionally found (**b**, arrowhead). **c**, **d**, Wild-type (WT, **c**) and *duf* (**d**) third instar garland cells. **c**, Diaphragms (arrowheads) and lacunae (red asterisks) densely populate the nephrocyte surface. **d**, *duf* nephrocytes have small lacunae (arrowheads) lacking diaphragms and a substantially thickened basement membrane (bm). **e**, **f**, Scanning electron micrographs of wild-type (**e**) and *duf* (**f**) third instar garland nephrocytes stripped of basement membrane by collagenase treatment. *duf* nephrocytes lack the furrows corresponding to diaphragm rows. **g**, **h**, Wild-type (**g**) and *duf* (**h**) Viking–GFP (collagen IV) third instar garland cells, stained with anti-GFP (green), showing greater Viking deposition around *duf* nephrocytes (arrowheads and inset). Garland cell number is also reduced in *duf* larvae, suggesting that mutant cells ultimately die. os, oesophagus; pv, proventriculus; tr, trachea. **i**, **j**, Diaphragm and foot process morphology are abnormal (arrowheads) in *sns* (**i**) and human *NPHS1* (**j**) embryonic overexpression. Scale bars: 200 nm (**a** (left), **c**, **d**), 100 nm (**a** (right), **b**), 50 nm (**i**, **j**) and 5 μm (**e**, **f**).

right)—possible remnants of undercoat normally associated with the wild-type diaphragm. These observations indicate that in the absence of the diaphragm, foot processes are unstable and undergo effacement. Scanning electron microscopy reveals the surface smoothing in mutant garland cells (compare Fig. 3e with Fig. 3f). These phenotypes are notably similar to those of podocytes lacking nephrin or NEPH1 (refs 5, 17). Thus, by analogy with nephrin and NEPH1 in the slit diaphragm, we suggest that Sns and Duf interact through their extracellular domains to form the nephrocyte diaphragm itself.

We noted that the basement membrane in *sns* knockdown and *duf* larval nephrocytes was irregular and markedly expanded (compare Fig. 3c to Fig. 3d). The basement membrane in *duf* nephrocytes has an average depth of 202 nm (±24 (s.e.m.), $n = 13$), compared with 57 nm (±4, $n = 11$) for the wild type. This results from an increase in deposition of the *Drosophila* collagen IV (Viking; Fig. 3g, h and Supplementary Fig. 3). However, this is unlikely to account for the fourfold thickening observed, and we suggest that a further contributing factor is accumulation of haemolymph proteins that clog the basement membrane owing to inefficient filtration.

Given the similarities between the morphology and molecular requirements for podocyte and nephrocyte diaphragms, we tested the ability of human *NPHS1* to rescue the *sns* mutant phenotype. However nephrocytes are sensitive to absolute levels of Sns, so even moderate overexpression produced abnormal phenotypes. We therefore compared the effects of overexpressing *Drosophila sns* with those of overexpressing human *NPHS1*. The resulting phenotypes are notably similar, including abnormal nephrocyte foot process morphology and marked thickening of diaphragm filaments (Fig. 3i, j). These data indicate that precise levels of Sns are critical for diaphragm formation and, more importantly, that human nephrin and *Drosophila* Sns function in equivalent ways.

Vertebrate nephrin and NEPH1 form a multi-protein complex at the slit diaphragm with zonula occludens-1 (ZO-1)[20], CD2-associated protein (CD2AP)[21,22] and podocin[23] (Supplementary Table 1). Mutations in these genes result in kidney disease[21,23,24]. We asked whether the fly orthologues (Supplementary Table 1) contribute to the nephrocyte diaphragm. *In situ* hybridization reveals that *pyd* (the orthologue of ZO-1), *CG31012* (CD2AP) and *Mec2* (*NPHS2*/podocin, Supplementary Fig. 4) are expressed in nephrocytes (Fig. 4a–f). Furthermore, Pyd–GFP (green fluorescent protein) precisely co-localizes with Duf to the membrane (Fig. 4g), mirroring co-localization of ZO-1 and NEPH1 in the podocyte[20].

Molecular interactions between these vertebrate slit-diaphragm-associated proteins have been established (Fig. 4h, black arrows)[11,20,22,25]. To test whether fly orthologues form a similar complex, we performed a yeast two-hybrid analysis with Sns and Duf intracellular domains (Fig. 4i). Sns interacts with Mec-2 (podocin) and Duf interacts with Pyd (ZO-1) (Fig. 4j). An interaction between Duf and Pyd was independently confirmed by co-immunoprecipitation (Fig. 4k). A previous report established direct association between Sns and Duf[26]. These interactions between the fly proteins (Fig. 4h, red arrows) closely resemble those described for slit-diaphragm-associated proteins (Fig. 4h, black arrows). These data, taken together with those described above, provide strong evidence that the nephrocyte diaphragm (Fig. 4l) and slit diaphragm are molecularly homologous structures.

Insect nephrocytes are size- and charge-selective in their sequestration of materials from the haemolymph. Selectivity is based on the characteristics of the diaphragm and basement membrane, which act together as a filtration barrier[7,9]. To test the filtration capacity of the *Drosophila* nephrocyte diaphragm, we assayed the passage of fluorescently labelled dextrans of different sizes. If the nephrocyte diaphragm acts as a size-selective filter, we reasoned that, like the vertebrate slit diaphragm[27], it would allow free passage of small (molecular mass of 10,000 Da) but exclude large (molecular mass of 500,000 Da) dextrans (Fig. 5b). In agreement with our expectations, uptake of the 500,000 Da dextran in wild-type nephrocytes is significantly lower than that of the 10,000 Da dextran (1:3.6, $n = 20$; Fig. 5a, f). These data strongly suggest that the nephrocyte diaphragm functions as a size-based filtration diaphragm (endocytosis from foot process tips could account for low levels of large dextran uptake, Fig. 5b). We anticipated higher uptake of the large dextran in immunoglobulin-domain mutant nephrocytes because they lack diaphragms. However, although the level of uptake of the small dextran in *duf* or *sns* nephrocytes is unaltered compared to wild type, we found a marked reduction in large dextran uptake (Fig. 5c, d, f); the large-to-small ratio is 1:22.5 ($n = 20$) for *duf* and 1:15.3 ($n = 19$) for *sns*. Instead, the large dextran appears as a halo surrounding the cell (Fig. 5c, d). The thickening of basement membrane observed in *duf* nephrocytes (Fig. 3d) could explain the exclusion of the large dextran (Fig. 5e). This highlights a further parallel between nephrocytes and podocytes. An endocytosis-based clearance mechanism in podocytes prevents clogging of the glomerular basement membrane with blood plasma proteins; the slit-diaphragm-associated protein CD2AP has been implicated in this process[24,28]. We suggest that an equivalent clearance mechanism exists in nephrocytes, and that this mechanism requires Sns and Duf.

Whatever the causes of reduction in filtration capability, the animal's haemolymph physiology will be disturbed. We tested this hypothesis by feeding larvae silver nitrate, a toxin endocytosed and concentrated in nephrocytes (Fig. 5h). At low concentrations of silver nitrate, viability of control larvae is not compromised (82% eclose as adults, Fig. 5i), but *duf* larvae show a greatly reduced viability (26% eclose, Fig. 5i). A previous study showed a requirement for nephrocytes in the face of toxic stress[29]. Our data show that immunoglobulin-domain proteins are essential for this function.

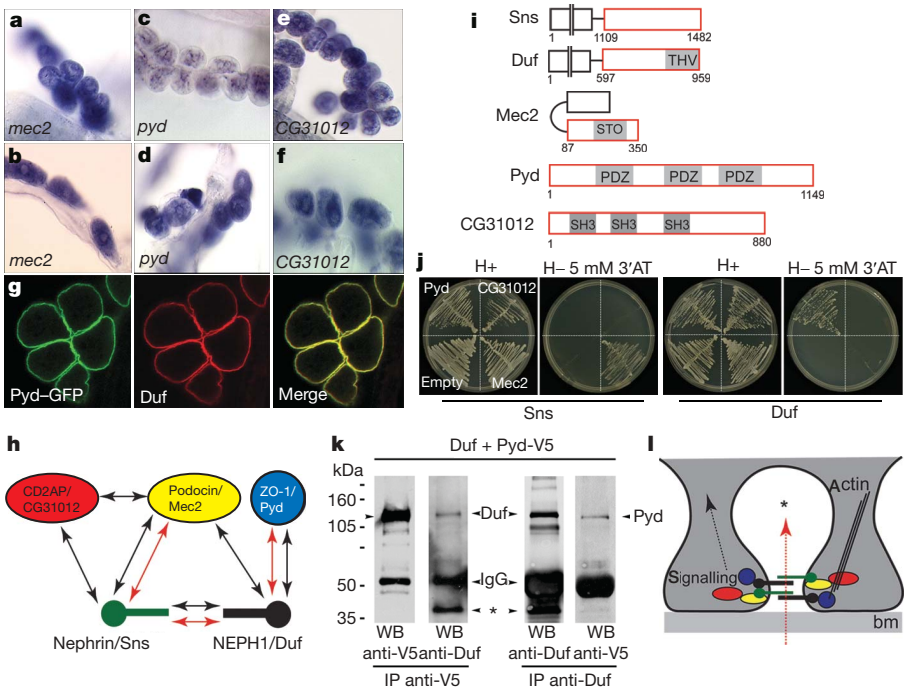

Figure 4 | Analysis of slit-diaphragm-associated protein orthologues in the fly nephrocyte. **a**–**f**, Third instar garland (**a**, **c**, **e**) and pericardial (**b**, **d**, **f**) nephrocytes hybridized with probes directed against *Mec2* (**a**, **b**), *pyd* (**c**, **d**) and *CG31012* (**e**, **f**). **g**, Pyd (left, green) and Duf (centre, red) co-localize (right, yellow) in third instar garland nephrocytes. **h**, Schematic of the main components of the podocyte slit diaphragm (black arrows) and nephrocyte diaphragm (described here and elsewhere, red arrows). **i**, Schematic of *Drosophila* orthologues of slit-diaphragm-associated proteins: PDZ-binding domain (THV), PDZ domain (PDZ), stomatin domain (STO) and SH3 domain (SH3). The region of the protein used in the yeast two-hybrid analysis is outlined in red. **j**, Yeast two-hybrid analysis of Sns or Duf with Pyd, CG31012, Mec2 and negative control (empty vector). Direct protein interaction is indicated by growth of yeast on selective media (H− 5 mM 3′AT). **k**, Duf and Pyd-V5 co-immunoprecipitate with each other from *Drosophila* cells (the unlabelled arrowhead on the left corresponds to Pyd; the asterisk indicates cleaved form of Duf that is also co-immunoprecipitated with Pyd). **l**, Schematic of molecular interactions at the nephrocyte diaphragm; Sns (green), Duf (black), Mec2 (yellow), Pyd (blue), CG31012 (red), direction of filtration (red arrow), extracellular lacuna (asterisk). Putative links to signalling or the actin cytoskeleton based on analogy with the equivalent complex at the slit diaphragm are shown. bm, basement membrane.

We have highlighted similarities between podocytes and nephrocytes; however, podocytes are an integral part of the nephron (Fig. 1a) whereas the nephrocyte is spatially separated from its renal (Malpighian) tubule (Fig. 1c). Such differences have contributed to the traditional view that vertebrate and invertebrate excretory systems are unrelated[1]. Nevertheless, nephron-like features are present

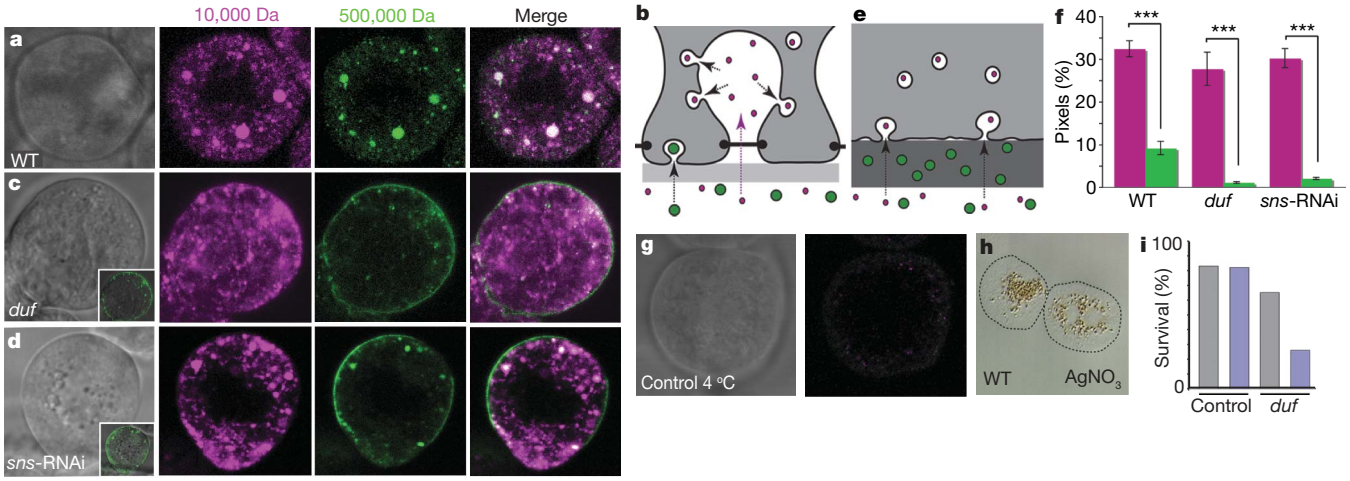

Figure 5 | Sns and Duf are required for nephrocyte filtration. **a**, **c**, **d**, Third instar garland nephrocytes from wild-type (WT, **a**), *duf* (**c**) and *sns*-RNAi knockdown (**d**) animals co-incubated with 10,000 Da (magenta) and 500,000 Da (green) fluorescently labelled dextran. Inset in **c** and **d** shows a merged image of transmitted light and 500,000 Da channels. **b**, **e**, Schematic drawing of filtration and endocytosis in wild-type (**b**) and *sns* or *duf* mutant (**e**) nephrocytes. **f**, Quantification of small (magenta) and large (green) dextran uptake in wild-type, *duf* and *sns*-RNAi knockdown garland cells. The percentage pixel number exceeding the threshold per unit area is shown on the *y*-axis (error bars, s.e.m.). Triple-asterisks indicate significance of $P < 0.001$. Please note, the molar ratio of dye to dextran is 1:1 (for 10,000 Da) and 64:1 (for 500,000 Da). **g**, A control nephrocyte incubated with fluorescent dextran at 4 °C showing no uptake (right image). **h**, Ten-micrometre section of garland nephrocytes from a wild-type larva fed with $AgNO_3$ (brown granular staining). **i**, The percentage of eclosing sibling control or *duf* adults fed yeast paste (grey) or yeast paste with $AgNO_3$ (blue; $n = 65$, 68, 55 and 57).

in the excretory systems of a wide variety of invertebrates and in the protochordate *Amphioxus*, suggesting a common origin[2]. The molecular parallels between nephrocytes and podocytes described here support this hypothesis, and it will be of interest to determine whether nephrin- and NEPH1-like protein complexes are found in other invertebrate filtration diaphragms.

Defects in the slit diaphragm complex underlie human diseases for which the unifying feature is proteinurea and kidney failure. These symptoms result from defective filtration, but in addition the nephrin–NEPH1 complex regulates podocyte behaviours such as cell survival, polarity, actin dynamics and endocytosis[30]. How these functions of the slit diaphragm relate to disease pathologies is currently unclear. The fly nephrocyte also depends on the activity of a nephrin–NEPH1 complex for survival, shape and selective endocytosis, and thus provides a simple and genetically tractable model in which the multiple roles of the slit diaphragm complex can be addressed.

METHODS SUMMARY

Fly strains. Flies were reared on standard food at room temperature (~22 °C), 18 °C or 25 °C. The strains used are listed in the Methods.

Nephrocyte filtration assay. Garland cells were dissected, incubated with AlexaFluor568-dextran (10,000 Da) and fluorescein-dextran (500,000 Da; Molecular Probes) at a concentration of 0.33 mg ml^{-1} at 25 °C for 5 min, washed on ice, fixed and mounted. Dextran uptake was quantified by counting the pixel number exceeding the background threshold per unit area using Volocity software.

Toxin stress assay. First instar larvae of the appropriate genotype were transferred to agar-only plates supplemented with yeast paste or with yeast paste containing $AgNO_3$ (2 g yeast in 3.5 ml of 0.003% $AgNO_3$), and allowed to develop at 25 °C. The percentage of eclosing adults was scored.

Antibodies. Antibodies used were: anti-Sns (1:200, from S. Abmayr), anti-Kirre (1:200, K. Fischbach), anti-Duf extracellular (1:50, M.R.-G.), anti-Duf intracellular (1:500, M.R.-G.), anti-βgal (1:1,000, ICN Biomedicals), anti-HRP (1:200, Jackson ImmunoResearch), anti-pericardin (1:2, DSHB) and anti-GFP (1:500, Invitrogen Molecular Probes).

Confocal and electron microscopy. Confocal and electron microscopy were carried out using standard techniques. For immuno-electron microscopy, dissected larval garland cells were fixed in 4% formaldehyde plus 0.05% glutaraldehyde, embedded in gelatin, cryosectioned, and incubated with anti-Duf extracellular (1:5), anti-Kirre (1:20) or anti-Sns (1:20) followed by 10 nm (for single stains) or both 5 nm and 10 nm (for double stains) gold-conjugated secondary antibody.

Yeast two-hybrid analysis. The intracellular domains of Sns and Duf were tested for interaction with Pyd (isoform f), CD2AP (SD08724) and the C-terminal cytoplasmic domain of Mec2 using the Clontech Matchmaker GAL4 two-hybrid system. Interaction was indicated by growth in the absence of histidine. 5 mM 3-amino-1,2,4-triazole (3′AT, Sigma) was included to titrate residual autoactivation from the bait fusion proteins.

Co-immunoprecipitation experiments. *Drosophila* S2 cells transiently co-transfected with pMK33/pMtHy-duf and pAC5.1V5-His-pyd were induced for 20 h with 0.7 mM $CuSO_4$. Total cell lysate was split and each half immunoprecipitated with either anti-V5 or anti-Duf intracellular antibodies and probed with anti-Duf intracellular antibodies and anti-V5 following standard protocols.

Full Methods and any associated references are available in the online version of the paper at www.nature.com/nature.

Received 4 August; accepted 8 October 2008.
Published online 29 October 2008.

1. Smith, H. W. *From Fish to Philosopher* (Little, Brown, 1953).
2. Ruppert, E. E. Evolutionary origin of the vertebrate nephron. *Am. Zool.* **34,** 542–533 (1994).
3. Rodewald, R. & Karnovsky, M. J. Porous substructure of the glomerular slit diaphragm in the rat and mouse. *J. Cell Biol.* **60,** 423–433 (1974).
4. Wartiovaara, J. *et al.* Nephrin strands contribute to a porous slit diaphragm scaffold as revealed by electron tomography. *J. Clin. Invest.* **114,** 1475–1483 (2004).
5. Patrakka, J. *et al.* Congenital nephrotic syndrome (NPHS1): features resulting from different mutations in Finnish patients. *Kidney Int.* **58,** 972–980 (2000).
6. Berridge, M. J. & Oschman, J. L. *Transporting Epithelia* 11–15 (Academic, 1972).
7. Crossley, A. C. in *Comprehensive Insect Physiology, Biochemistry and Pharmacology* (eds Kerkut, G. A. & Gilbert, L. I.) 487–515 (Pergamon, 1985).
8. Kowalevsky, A. Ein Beitrag zur Kenntnis der Excretions-organe. *Biol. Centralbl.* **9,** 74–79 (1889).
9. Locke, M. & Russell, V. W. in *Microscopic Anatomy of Invertebrates* (eds Harrison, F. W. & Locke, M.) 687–709 (Wiley, 1998).
10. Kestila, M. *et al.* Positionally cloned gene for a novel glomerular protein—nephrin—is mutated in congenital nephrotic syndrome. *Mol. Cell* **1,** 575–582 (1998).
11. Sellin, L. *et al.* NEPH1 defines a novel family of podocin interacting proteins. *FASEB J.* **17,** 115–117 (2003).
12. Ruotsalainen, V. *et al.* Nephrin is specifically located at the slit diaphragm of glomerular podocytes. *Proc. Natl Acad. Sci. USA* **96,** 7962–7967 (1999).
13. Gerke, P., Huber, T. B., Sellin, L., Benzing, T. & Walz, G. Homodimerization and heterodimerization of the glomerular podocyte proteins nephrin and NEPH1. *J. Am. Soc. Nephrol.* **14,** 918–926 (2003).
14. Barletta, G. M., Kovari, I. A., Verma, R. K., Kerjaschki, D. & Holzman, L. B. Nephrin and Neph1 co-localize at the podocyte foot process intercellular junction and form *cis* hetero-oligomers. *J. Biol. Chem.* **278,** 19266–19271 (2003).
15. Khoshnoodi, J. *et al.* Nephrin promotes cell–cell adhesion through homophilic interactions. *Am. J. Pathol.* **163,** 2337–2346 (2003).
16. Liu, G. *et al.* Neph1 and nephrin interaction in the slit diaphragm is an important determinant of glomerular permeability. *J. Clin. Invest.* **112,** 209–221 (2003).
17. Donoviel, D. B. *et al.* Proteinuria and perinatal lethality in mice lacking NEPH1, a novel protein with homology to NEPHRIN. *Mol. Cell. Biol.* **21,** 4829–4836 (2001).
18. Tepass, U. & Hartenstein, V. The development of cellular junctions in the *Drosophila* embryo. *Dev. Biol.* **161,** 563–596 (1994).
19. Rugendorff, A., Younossi-Hartenstein, A. & Hartenstein, V. Embryonic origin and differentiation of the *Drosophila* heart. *Rouxs Arch. Dev. Biol.* **203,** 266–280 (1994).
20. Huber, T. B. *et al.* The carboxyl terminus of Neph family members binds to the PDZ domain protein zonula occludens-1. *J. Biol. Chem.* **278,** 13417–13421 (2003).
21. Shih, N. Y. *et al.* Congenital nephrotic syndrome in mice lacking CD2-associated protein. *Science* **286,** 312–315 (1999).
22. Shih, N. Y. *et al.* CD2AP localizes to the slit diaphragm and binds to nephrin via a novel C-terminal domain. *Am. J. Pathol.* **159,** 2303–2308 (2001).
23. Boute, N. *et al.* NPHS2, encoding the glomerular protein podocin, is mutated in autosomal recessive steroid-resistant nephrotic syndrome. *Nature Genet.* **24,** 349–354 (2000).
24. Kim, J. M. *et al.* CD2-associated protein haploinsufficiency is linked to glomerular disease susceptibility. *Science* **300,** 1298–1300 (2003).
25. Schwarz, K. *et al.* Podocin, a raft-associated component of the glomerular slit diaphragm, interacts with CD2AP and nephrin. *J. Clin. Invest.* **108,** 1621–1629 (2001).
26. Galletta, B. J., Chakravarti, M., Banerjee, R. & Abmayr, S. M. SNS: Adhesive properties, localization requirements and ectodomain dependence in S2 cells and embryonic myoblasts. *Mech. Dev.* **121,** 1455–1468 (2004).
27. Kramer-Zucker, A. G., Wiessner, S., Jensen, A. M. & Drummond, I. A. Organization of the pronephric filtration apparatus in zebrafish requires Nephrin, Podocin and the FERM domain protein Mosaic eyes. *Dev. Biol.* **285,** 316–329 (2005).
28. Akilesh, S. *et al.* Podocytes use FcRn to clear IgG from the glomerular basement membrane. *Proc. Natl Acad. Sci. USA* **105,** 967–972 (2008).
29. Das, D., Aradhya, R., Ashoka, D. & Inamdar, M. Post-embryonic pericardial cells of *Drosophila* are required for overcoming toxic stress but not for cardiac function or adult development. *Cell Tissue Res.* **331,** 565–570 (2008).
30. Huber, T. B. & Benzing, T. The slit diaphragm: a signaling platform to regulate podocyte function. *Curr. Opin. Nephrol. Hypertens.* **14,** 211–216 (2005).

Supplementary Information is linked to the online version of the paper at www.nature.com/nature.

Acknowledgements We thank F. Evers, Z. Cseresnyes, M. Guerra and E. Salvador for technical assistance, and S. Abmayr, L. Cooley, C. Doe, M. Affolter, K. Fischbach and K. Tryggvason for reagents. We thank V. Hartenstein, M. Inamdar, A. Woolf, I. Miguel-Aliaga, F. Evers, M. Landgraf and members of the Skaer laboratory for discussions, and E. Knust and W. B. Huttner for their support. This work was supported by Wellcome Trust grants awarded to H.S. (072441 and 079221; H.W., B.D. and H.S.); Deutsche Forschungsgemeinschaft SFB 590 awarded to E. Knust (F.G.) and ARC 1242 (H.W., B.D., H.S. and F.G.); an MEC grant awarded to M.R.-G. (BFU2007-62201; S.P.-S. and M.R.-G.); a Fundación Ramón Areces grant to the CBMSO (M.R.-G.); EC grant LSHG-CT-2004-511978 to MYORES (M.R.-G.); and an FPU fellowship from the MEC awarded to A.G.-L.

Author Contributions B.D., H.S. and M.R.-G. designed and directed the project. B.D., H.W., M.R.-G. and S.P.-S. performed the experiments. F.G. and M.W.-B. provided technical assistance. A.G.-L. and R.A. provided materials. B.D. and H.S. wrote the paper. All authors discussed results and commented on the manuscript.

Author Information Reprints and permissions information is available at www.nature.com/reprints. Correspondence and requests for materials should be addressed to H.S. (hs17@cam.ac.uk).

METHODS

Fly strains. The following fly genotypes were used: OregonR (wild-type strain); sns^{XB3} and *UAS-sns* (gift from S. Abmayr); $Df(1)w^{67k30}$ hemizygotes for embryonic analysis of *duf*; $Df(1)w^{67k30}/Df(1)N^{5419}$ transheterozygotes or $Df(1)duf^{ps\text{-}1}$ (small deficiency removing the *duf* locus only, a description of this allele will be published elsewhere, S.P.-S. *et al.*, in preparation) for larval analysis of *duf*; *rP298* (*duf-LacZ*); *UAS-Pyd-GFP* (gift from M. Affolter); *Viking-GFP* (gift from L. Cooley); *UAS-sns-RNAi* (a 1,047 bp fragment was obtained by PCR from *sns* complementary DNA using primers 5′-CCAGTTCGTATAATGACACCG-3′ and 5′-CCTACAGCTATACGAGGTGTC-3′ and used to make intron-spliced hairpin RNA according to ref. 31); *UAS-NPHS1* (human *NPHS1* cDNA, gift from K. Tryggvason, cloned into pUAST); *G447.2-GAL4* (embryonic garland cell driver; gift from R. Reuter); and *Prospero-Gal4* (larval garland cell driver; gift from C. Doe). Fly crosses were maintained at 25 °C except for the overexpression experiment in which animals were maintained at 29 °C to ensure maximum transgene expression. Marked balancer chromosomes (Krüppel–Gal4, UAS–GFP) and/or PCR genotyping[32] from carcasses remaining after dissection were used to identify appropriate genotypes.

Nephrocyte filtration assay. Garland nephrocytes (including a small portion of oesophagus and the proventriculus) were dissected from third instar larvae in Shields and Sang medium (Sigma), and were then transferred to media containing AlexaFluor568-dextran (10,000 Da) and fluorescein-dextran (500,000 Da; Molecular Probes) at a concentration of 0.33 mg ml^{-1}, and incubated at 25 °C for 5 min. The cells were washed on ice for 10 min in cold PBS, fixed in 4% formaldehyde for 10 min at room temperature (~22 °C), rinsed once in PBS and then mounted in vectashield (Vector labs). All post-dissection procedures were carried out in the dark. A single confocal section of the cell midpoint was taken using a Leica SP1 confocal microscope, and dextran uptake was quantified by counting the pixel number exceeding the background threshold per unit area using Volocity software. The average fluorescence from the proventriculus epithelium (where dextran uptake does not occur) was used to set the background threshold. The same threshold was used for all experiments. Control cells incubated with dextran on ice showed no uptake. Results were analysed statistically using the Shapiro–Wilk normality test followed by the paired *t*-test or Kruskal–Wallis Rank Sum test as appropriate.

Toxin stress assay. Flies of the appropriate genotype were allowed to lay on standard apple juice plates supplemented with yeast. After approximately 24 h, freshly emerging first instar larvae from this plate were transferred to agar-only plates supplemented with yeast paste or with yeast paste containing $AgNO_3$ (2 g yeast in 3.5 ml of 0.003% $AgNO_3$), and allowed to develop at 25 °C. The percentage of eclosing adults was scored.

***In situ* hybridization and immunohistochemistry.** Whole-mount *in situ* hybridization and immunohistochemistry to embryos and third instar nephrocytes were carried out using standard techniques. Antibodies used were: anti-Sns (1:200, gift from S. Abmayr), anti-Kirre (1:200, gift from K. Fischbach), anti-Duf extracellular (1:50), anti-Duf intracellular (1:500, the generation of both antisera will be published elsewhere), anti-βgal (1:1,000, ICN Biomedicals), anti-HRP (1:200, Jackson ImmunoResearch), anti-pericardin (1:2, DSHB), anti-GFP (1:500, Invitrogen Molecular Probes), AlexaFluor 488 phalloidin and AlexaFluor 568 phalloidin (1:20, Invitrogen Molecular Probes), and TOTO3 and TO-PRO-3 (1:100, Invitrogen Molecular Probes).

Confocal and electron microscopy. Confocal microscopy, transmission electron microscopy and scanning electron microscopy were carried out using standard techniques. For immuno-electron microscopy, dissected garland cells were fixed in 4% formaldehyde plus 0.05% glutaraldehyde, embedded in gelatin, and cryosectioned and incubated with anti-Duf extracellular (1:5), anti-Kirre (1:20), or anti-Sns (1:20) followed by 10 nm (for single stains) or both 5 nm and 10 nm (for double stains) gold-conjugated secondary antibody. In some cases, confocal images correspond to *z*-projections from a series of confocal sections.

Collagenase treatment. Third instar garland cells were incubated in 0.1% collagenase type I in PBS for 3 min at 37 °C.

Yeast two-hybrid assays. The intracellular domains of Sns and Duf were used as bait (cloned into pGBKT7, Clontech) and tested for interaction with Pyd (isoform f), CD2AP (SD08724), and C-terminal cytoplasmic domain of Mec2 (all cloned into pGADT7, Clontech). Interaction was indicated by growth in absence of histidine. 5 mM 3′AT (Sigma) was included to titrate residual auto-activation from the bait fusion proteins.

Co-immunoprecipitation experiments. *Drosophila* S2 cells transiently co-transfected with pMK33/pMtHy-duf and pAC5.1V5-His-pyd were induced for 20 h with 0.7 mM $CuSO_4$. Total cell lysate was split and each half immunoprecipitated with either anti-V5 or anti-Duf, and probed consecutively with anti-Duf and anti-V5 or anti-V5 and anti-Duf, respectively, following standard protocols.

31. Nagel, A. C., Maier, D. & Preiss, A. Green fluorescent protein as a convenient and versatile marker for studies on functional genomics in *Drosophila*. *Dev. Genes Evol.* **212**, 93–98 (2002).
32. Strunkelnberg, M. *et al. rst* and its paralogue *kirre* act redundantly during embryonic muscle development in *Drosophila*. *Development* **128**, 4229–4239 (2001).